Polymineralic orientation analysis of magmatic rocks using Electron Back-Scatter Diffraction: Implications for igneous fabric origin and evolution

I. Romeo [a,*], R. Capote [b], R. Lunar [c], N. Cayzer [d]

[a] *Department of Geology, University of California Davis, One Shields Avenue, Davis, CA 95616-8605 USA*
[b] *Departamento de Geodinámica, Facultad de Ciencias Geológicas, Universidad Complutense de Madrid, 28040 Madrid, Spain*
[c] *Departamento de Cristalografía y Mineralogía, Facultad de Ciencias Geológicas, Universidad Complutense de Madrid, 28040 Madrid, Spain*
[d] *School of GeoSciences, University of Edinburgh, Kings Buildings, West Mains Road, Edinburgh EH9 3JW, United Kingdom*

Abstract

Electron Back-Scatter Diffraction (EBSD), which provides an easy way of acquiring large numbers of individual crystallographic orientation data from different phases, has been applied to the study of magmatic fabrics. Using this technique, the crystallographic preferred orientation (CPO) of plagioclase, biotite, orthopyroxene, hornblende and quartz in natural tonalites and quartzdiorites (from the Santa Olalla Igneous Complex, SW Iberia) deformed during the magmatic stage have been determined. Plagioclase is the coarser phase defining the main fabric in each sample, whereas biotite can display either the same fabric as plagioclase or a completely different one. The differences between these two phases occur because: (1) smaller phases interact with the larger ones to produce more random orientations, (2) under simple shear, finer phases can completely rotate giving a girdle included in the XZ plane, (3) finer phases can more easily preserve relict fabrics, while the coarser phases are completely reoriented by the last stress tensor. The last phases to crystallize show weak to completely random CPOs (hornblende) or completely random distributions (quartz). The study was completed with a shape preferred orientation analysis using the Intercept Method in order to detect weak magmatic lineations, and numerical modelling simulations of theoretically equivalent simple shear situations for each sample.

Keywords: Crystallographic preferred orientation (CPO); Shape preferred orientation (SPO); Magmatic fabrics; Structural geology

1. Introduction

Electron Back-Scatter Diffraction (EBSD) is a useful technique for determining crystallographic preferred orientations (CPO) of minerals (Prior et al., 1999). This technique has allowed the resolution of a number of geological problems related to ductile deformation in mylonites (Bestmann et al., 2004; Ji et al., 2004; Llana-Fúnez and Rutter, 2005; among others), misorientation analysis (Fliervoet et al., 1999; Pennock et al., 2005; among others) and crystallography (Kogure and Bunno, 2004; Kameda et al., 2005; among others). The potential usefulness of EBSD to study the formation and evolution of plutonic fabrics was suggested by Prior et al. (1999), but this technique has not previously been applied to

* Corresponding author. Tel. +1 510 705 30 55.
E-mail addresses: romeo@geology.ucdavis.edu (I. Romeo), capote@geo.ucm.es (R. Capote), lunar@geo.ucm.es (R. Lunar), Nicola.Cayzer@ed.ac.uk (N. Cayzer).

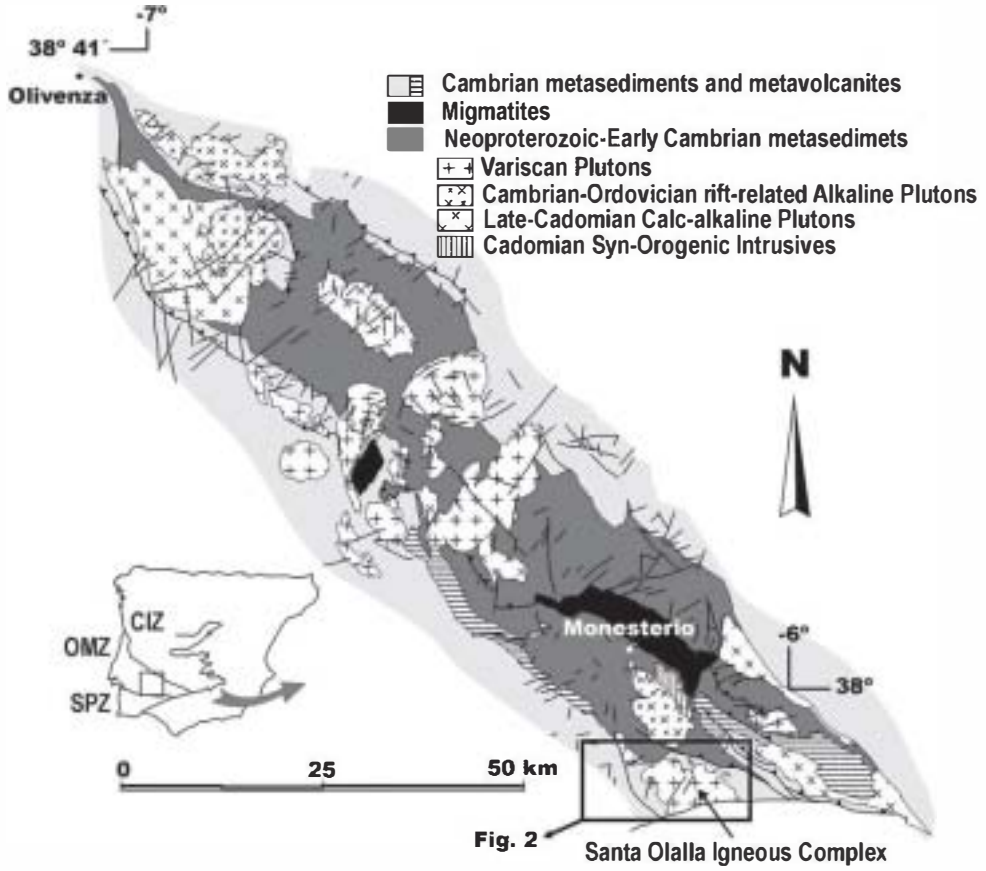

Fig. 1. Geological setting of the study area in the Olivenza-Monesterio antiform. Inset: location in the Iberian Massif (CIZ: Centroiberian Zone, OMZ: Ossa-Morena Zone, SPZ: South Portuguese Zone).

magmatic fabrics in granitoids, although it has been successfully applied to constraint fabrics in basaltic lava flows (Bascou et al., 2005). The capacity of EBSD to yield a large number of precise crystallographic orientations of different mineral phases very rapidly facilitates the determination of CPOs, even when these are weak, as occurs in magmatic rocks.

Plutonic rocks usually show a preferred orientation of minerals formed during deformation in the magmatic state (magmatic fabrics, Paterson et al., 1989; Park and Means, 1996; Paterson et al., 1998) and sometimes due to sub-solidus deformation (deformational fabrics, Paterson et al., 1989; Vernon et al., 2004). The formation of magmatic preferred orientation has been studied from analog experiments (Fernandez, 1987; Ildefonse et al., 1992; Arbaret et al., 1996, 2000), numerical modelling (Willis, 1977; Jezek et al., 1994; Arbaret et al., 2000; Iezzi and Ventura, 2002; Launeau, 2004), and natural samples (Blumenfeld, 1983; Blumenfeld and Bouchez, 1988; Benn and Allard, 1989; Pignotta and Benn, 1999). Numerical modelling shows that the final fabric geometry depends on the type of deformation (coaxial, non-coaxial, or a mixture of both) and the geometry of the particles that register the strain. Numerical simulations are based on the formulae developed by Jeffery (1922) that describe the motion of ellipsoidal rigid particles rotating into a melt under different strain conditions. A development of the Jeffery theory was performed by Arbaret et al. (2000), Fernandez et al. (1983), Launeau (2004), and Willis (1977), yielding periodic rotation of the particles deformed by simple shear, and the development of a shape preferred orientation (SPO) periodically parallel to the shear plane. These models differ from the magmatic process, mainly because they do not consider the interactions between adjacent particles (Ildefonse et al., 1992; Tikoff and Teyssier, 1994; Arbaret et al., 1996). The interactions between large and flat crystals deformed under simple shear generate an imbrication or tiling (Blumenfeld, 1983; Blumenfeld and Bouchez,

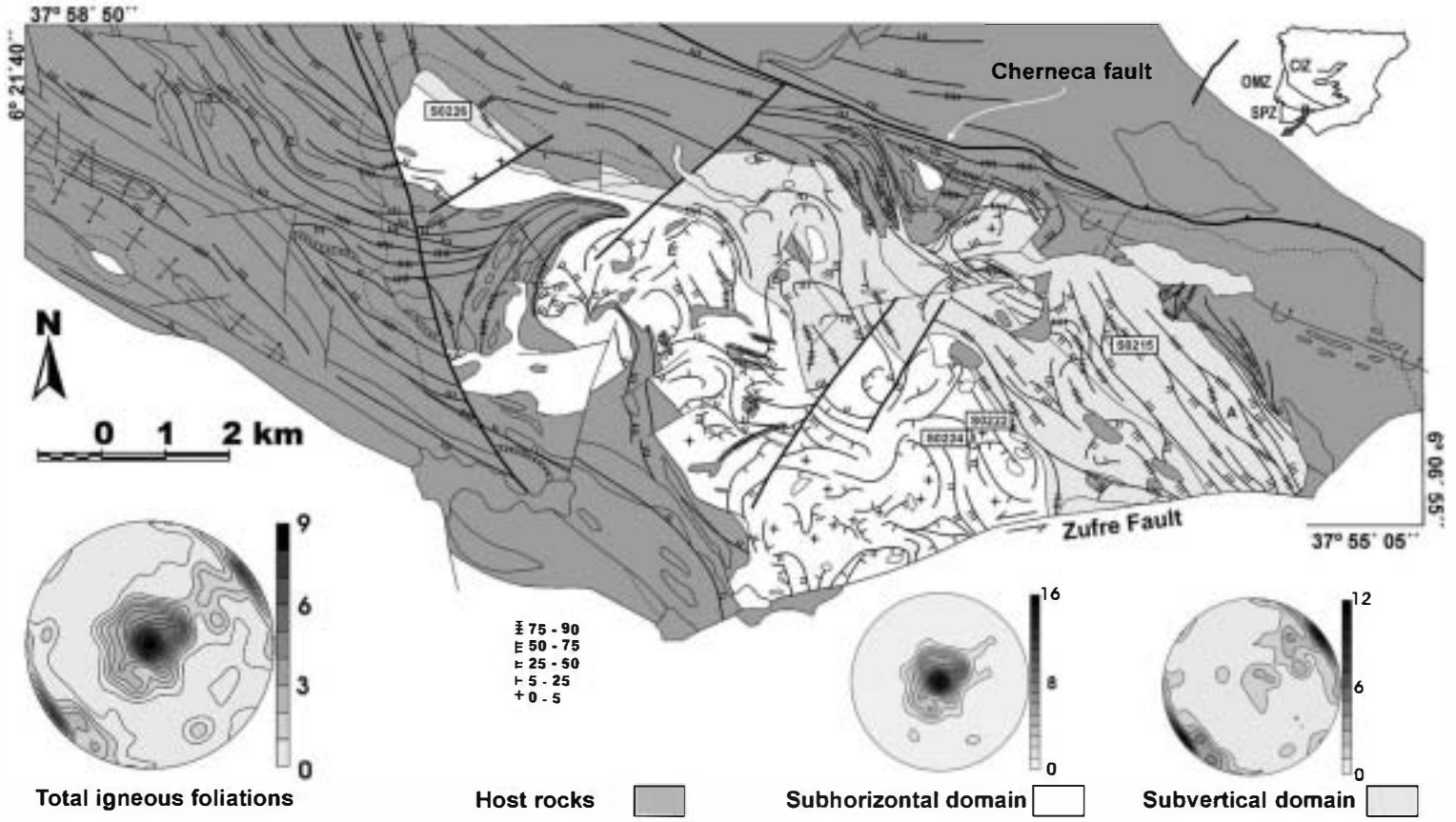

Fig. 2. Magmatic foliation map and stereoplots of the Santa Olalla Igneous Complex. A) Sinistral S–C patterns indicated by the foliation trajectories. The location of the samples analyzed by EBSD is shown.

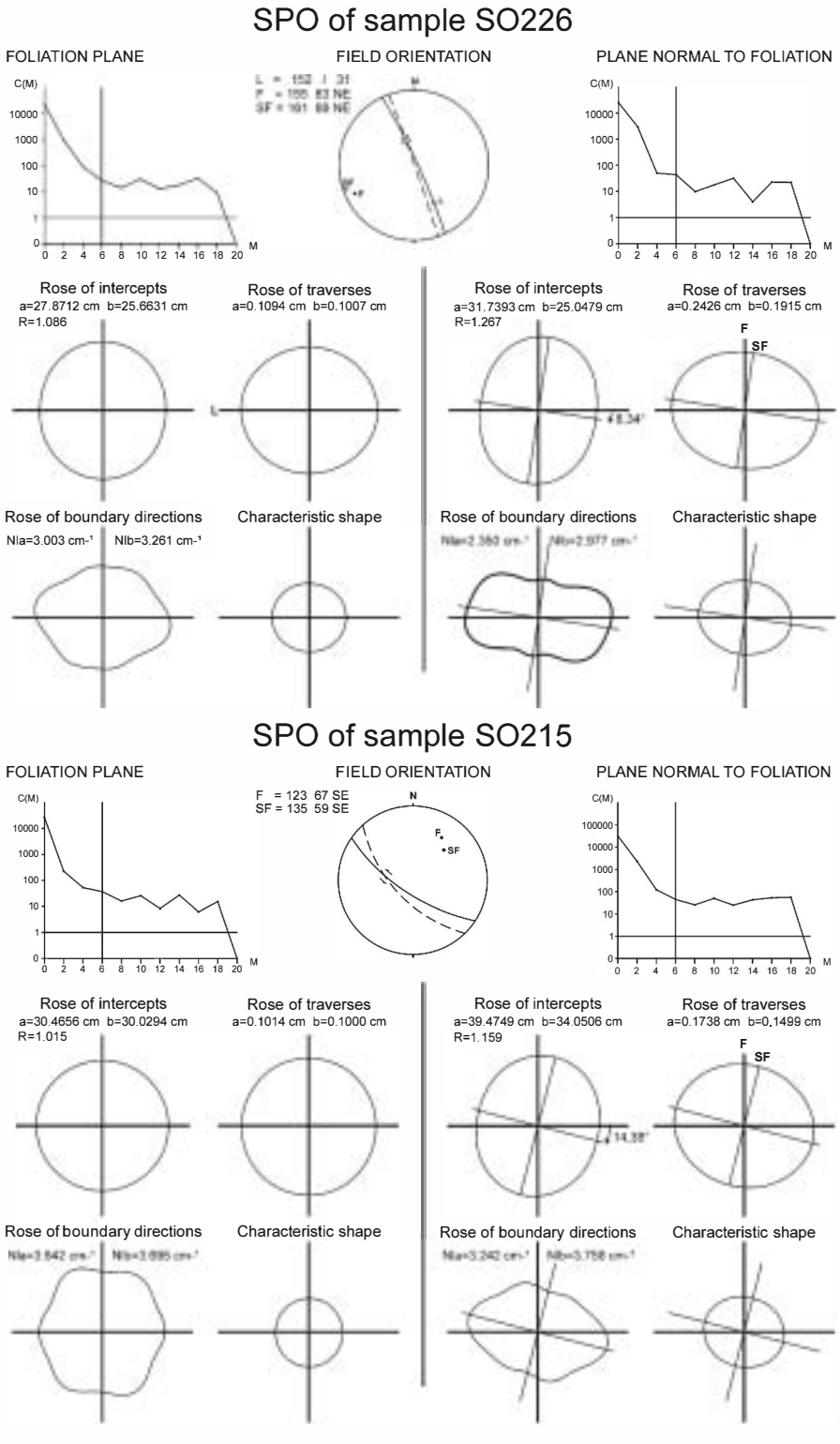

Fig. 3. SPO study of plagioclase grains performed by the intercept method on samples from the subvertical structural domain (SO226 and SO215), with the Fourier series truncation at F_6. The results were obtained by using the freeware "Intercepts 2003". The rose of intercepts, the rose of traverses, the rose of boundary directions and characteristic shape are shown for a section within the foliation plane and a section normal to foliation. The field orientation of the fabric elements (F: mesoscopic foliation, SF: shape foliation, and L: shape lineation) is shown in an equal-angle stereographic projection.

1988; Ildefonse et al., 1992; Arbaret et al., 1996) yielding a fabric with monoclinic symmetry which can be used as a shear sense indicator.

During the magma cooling consecutively different mineral phases start to crystallize. If magma suffers any stress (tectonic stress, internal stress caused by magmatic flow during emplacement, or filter pressing and porous flow during crystallization, Paterson et al., 1998) the first phases to crystallize can easily be oriented forming a magmatic fabric. The first phases crystallizing are growing into a liquid, consequently they show euhedral shapes controlled by their internal crystallographic structure. This relates the SPO with the CPO in the first-crystallizing mineral phases. In the study presented below, a CPO has been determined for minerals formed during the crystallizing sequence in a plutonic rock, from the first formed and well oriented phases to the last-crystallized, usually poikilitic and randomly oriented phases. The study was performed on the Santa Olalla Igneous Complex (SOIC), a well known, late-Variscan plutonic group located in the Olivenza-Monesterio antiform, a major structure in the Ossa Morena Zone, SW Iberia (Fig. 1). The geometry at depth of this plutonic complex and the orientation of their internal fabrics is well constrained since the study by Romeo et al. (2006b). We chose this plutonic complex to apply the EBSD technique because their emplacement mechanism was already established.

The SOIC is formed by two main plutons: the larger Santa Olalla stock and the Aguablanca stock. The Santa Olalla stock (Eguiluz et al., 1989) comprises amphibole–biotite quartz–diorite in the northern area grading into a main tonalitic facies in the centre that passes to a small body of monzogranite towards the southern limit. Towards the NW there is a mafic apophysis called Sultana, composed of hornblende–biotite tonalite and quartz–diorite. In the northern part of the complex is the Aguablanca stock, a mafic subcircular pluton (Romeo et al., in press). This is composed of phlogopite-rich gabbro–norite and norite grading southwards into diorite. On the north margin of the Aguablanca stock an Ni–Cu–PGE ore deposit has been recently discovered (Lunar et al., 1997; Tornos et al., 1999, 2001; Ortega et al., 2004; Piña et al., 2006). Some late-intruded granites complete the igneous intrusive sequence. The geochronology of the complex is constrained since the U–Pb results obtained by Romeo et al. (2006a) yielding ages within the interval of 340±3 Ma. These ages are similar to other plutons dated in the Olivenza-Monesterio antiform (Dallmeyer et al., 1995; Bachiller et al., 1997; Casquet et al., 1998; Montero et al., 2000), defining a main Variscan magmatic event, lasting from 353 to 329 Ma.

The SOIC is located in a wedge limited by two main sinistral faults: the Cherneca Fault (Romeo et al., 2007a) trending parallel to the general Variscan direction in this zone (N120°) with a reverse and sinistral kinematics, and the Zufre fault, a late-Variscan N80° sinistral strike–slip fault.

2. Methodology

2.1. Shape preferred orientation (SPO) determined using the Intercept method

Magmatic foliations are evident at the mesoscale indicated by the parallelism of plagioclase crystals and can be used to establish the framework of each sample. The fabric will be analyzed in detail by determining the CPO of each mineral, but in order to completely constraint the framework of each sample a determination of a possible magmatic lineation is needed. Magmatic lineations in our samples are so weak that they cannot be directly determined at the mesoscale, so we need a special technique to determine if they exist and how are they oriented.

The intercept method (Launeau and Robin, 1996) has been applied with the aim of constraining the magmatic shape fabric of plagioclase (the main oriented mineral in our samples). This technique allows us to detect the orientation of magmatic lineations in our samples even if they are very weak, which has been very useful for interpreting the CPO study in the correct framework for each sample.

The intercept method has been applied using the freeware "Intercepts 2003" created by Patrick Launeau and Pierre-Yves F. Robin. The method is based on counting the number of intercepted grain boundaries on a 2-dimensional image by a set of parallel scan lines along a number of directions. The resulting rose of intercept counts can be decomposed into a Fourier series, which can then be used to extract a rose of directions and a characteristic shape. For more details concerning this method see Launeau and Robin (1996). The orientation of the shape fabric ellipse for each of the studied sections was obtained together with the intensity of the shape fabric which is determined by R (eccentricity of the shape fabric ellipse).

2.2. Crystallographic preferred orientation (CPO) determined by Electron Back-Scatter Diffraction (EBSD)

In a scanning electron microscope (SEM) an electron beam creates an omni-directional source of scattered electrons within a specimen. Diffraction of these electrons will occur simultaneously on all lattice planes in the sample and the backscattered electrons, which escape

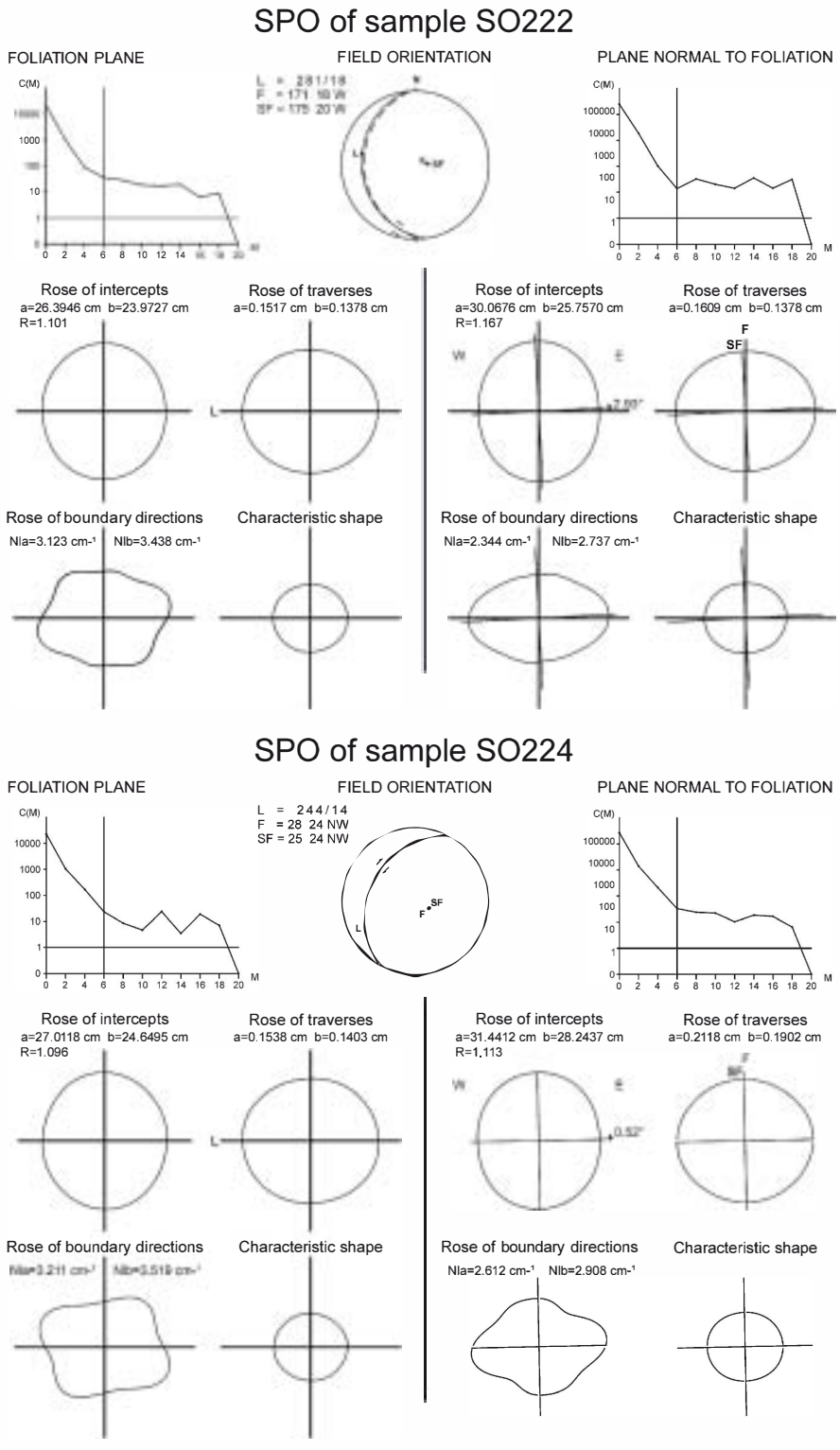

Fig. 4. SPO study of plagioclase grains performed by the intercept method on samples from the subhorizontal structural domain (SO222 and SO224), with the Fourier series truncation at F_6. The results were obtained by using the freeware "Intercepts 2003". The rose of intercepts, the rose of traverses, the rose of boundary directions and characteristic shape are shown for a section within the foliation plane and a section normal to foliation. The field orientation of the fabric elements (F: mesoscopic foliation, SF: shape foliation, and L: shape lineation) is shown in an equal-angle stereographic projection.

from the specimen, will form a diffraction pattern that can be imaged on a phosphor screen. This is the basis of Electron Back-Scatter Diffraction (EBSD) (Prior et al., 1999). Similar diffraction effects cause individual grains of different orientations to give different total back-scattered electrons. EBSD enables measurement of the crystallographic orientation of individual rock-forming minerals as small as 1 μm.

The EBSD analyses were obtained using an HKL Channel5 EBSD system on a Philips XL30CP SEM housed in the School of GeoSciences, University of Edinburgh. While EBSD analyses can be collected automatically, performing a grid of measurements with a regular spacing, this automatic mapping method was rejected due to the high number of phases to index. The analyses were collected manually, one by one, a procedure that allows to check the correct indexing of each electron back-scatter pattern for each previously recognized phase. Manual mapping completely covered the thin section surface in order to take the all the grains available in each sample. The number of analysis performed for each phase and sample, N, is reported in each diagram (Figs. 5–8).

3. Igneous structure

An explanation of the orientation of the magmatic foliations at the mesoscale is required before we present the results of our fabric study in order to understand the structural location of each analyzed sample.

The SOIC was deformed during the magmatic phase, and no evidence of important sub-solidus strain has been found. Only quartz shows a weak sub-solidus deformation characterized by undulose extinction and subgrains, while plagioclase, biotite, and hornblende remain undeformed. The tonalite, quartzdiorite and gabbronorite show preferred orientations of plagioclase (1–4 mm long) forming magmatic foliations favoured by the planar habit of this mineral. These mesoscopic magmatic foliations were mapped, (Fig. 2) revealing a consistent orientation pattern in which two different structural domains can be distinguished: an NE area trending parallel to the long axis of the stock, where the foliations show dominantly an NW–SE trend and vertical or high dip angle foliations, and the SW area where foliations are dominantly of low dip angle or horizontal (see stereo plots shown in Fig. 2).

The vertical N140° striking structural domain of the NE margin is concordant with the structural trajectories of the host rock. The vertical foliations show two main directions: bands (100–200 m wide) with an N130° strike and dipping 90° to 70° to the south and, between those bands, foliations quite oblique with an N155° trend and vertical dips. In the foliation trajectory map this pattern outlines rhomboidal shapes (A in Fig. 2) that were interpreted as kilometre-scale S–C structures (Romeo et al., 2006b).

The sub-horizontal structural domain in the SW shows that magmatic foliations are dominantly discordant with respect to the intrusive contact, but the host rock structure is dominantly parallel to the pluton margins. The transition between both domains is mainly characterized by narrow bands with vertical foliations striking N155° that appear to cut the surrounding horizontal fabrics. With respect to the relationships with the main faults it can be deduced that the Zufre fault has a clear post-intrusive character as it cuts all the foliations in the tonalite, unlike the Cherneca fault which runs parallel to the subvertical domain of the SOIC.

An extensive structural analysis combined with gravity modelling has been recently performed (Romeo et al., 2006b) giving an interpretation of the emplacement mechanism and tectonic evolution during cooling, that can be summarised as follows. First, during the syntectonic sinistral movement of the Cherneca fault the ascent of magma took place favoured by the generation of vertical pull-apart inter-connected gaps along this structure. When magmas reach its final level of emplacement a horizontal sheet-like intrusion started to propagate towards the SW generating the subhorizontal structural domain parallel to the upper and lower magma host rock contacts. Stoping also played an important role allowing a moderate ascent of the magma in the last stages of emplacement. Continuous motion along the Cherneca fault produced the sinistral shear deformation in a magmatic state of the NE portion of the Santa Olalla Igneous Complex, which generated a superimposed vertical fabric with sinistral kilometric-scale S–C magmatic structures. Finally, after complete crystallization of the magma at this shallow depth, the rheology of tonalite was too strong for deformation to proceed under sub-solidus conditions. As a consequence, the wide shear deformation zone allowed by melt rheology, was again restricted to the initial fault trace. Some time later, the Zufre fault cut across the Santa Olalla Igneous Complex, displacing its SE portion below the present erosion level.

4. Fabric study

The Santa Olalla tonalite was sampled in order to study the magmatic fabric in detail. Four samples were analyzed by the Intercept Method and EBSD: 2 from the subhorizontal domain (SO222 and SO224) and 2 from the subvertical domain (SO215 and SO226), the locations are shown in Fig. 2.

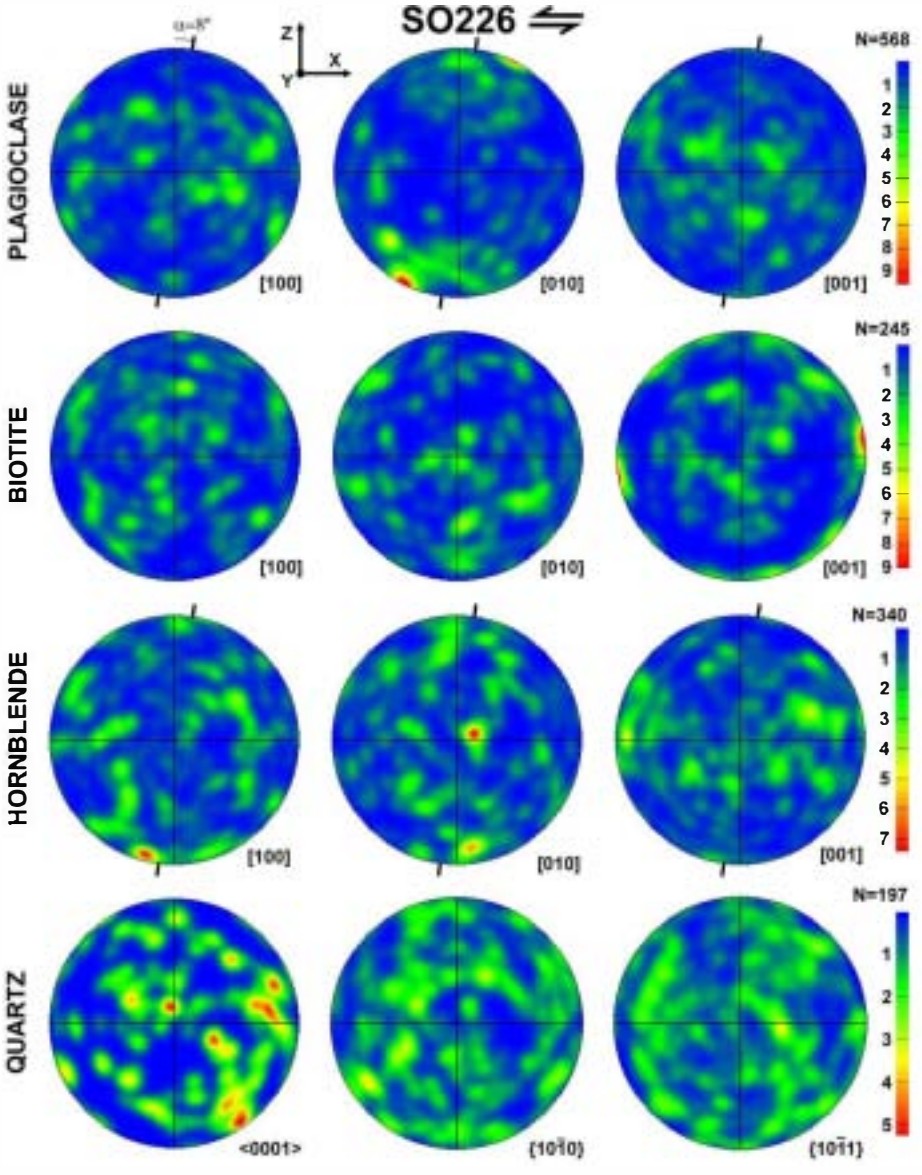

Fig. 5. Lower hemisphere equal-area projections of the CPOs of plagioclase, biotite, hornblende and quartz for the samples SO226 (subvertical domain) obtained by EBSD. The plane XY corresponds to the measured mesoscopic foliation and X to the lineation obtained in the SPO study of plagioclase. The α angle of plagioclase is indicated. *N* is the number of EBSD measurements. The units of the scale bars are multiples of random distribution.

4.1. Shape preferred orientation

For each sample two images were analyzed by the intercept method. One image corresponding to a section normal to foliation and the other within the foliation plane. The image perpendicular to foliation allows us to infer the intensity of the planar fabric of each sample, while the image parallel to foliation indicates the direction and intensity of the magmatic lineation if present.

The mineral used for the SPO study was plagioclase because it is the main fabric forming phase in all the samples. The images were obtained by scanning thin sections, these images were then processed in order to identify with a unique colour for the plagioclase. Finally, the obtained images were analyzed by the freeware "Intercepts 2003" with the Fourier series truncation at F_6, obtaining the following results (Figs. 3, 4).

4.1.1. Subvertical domain (SO226, SO215)

The SPO analysis of sample SO226 is shown in Fig. 3. It has revealed a magmatic lineation with a subhorizontal orientation (31° of immersion). The SPO obtained within

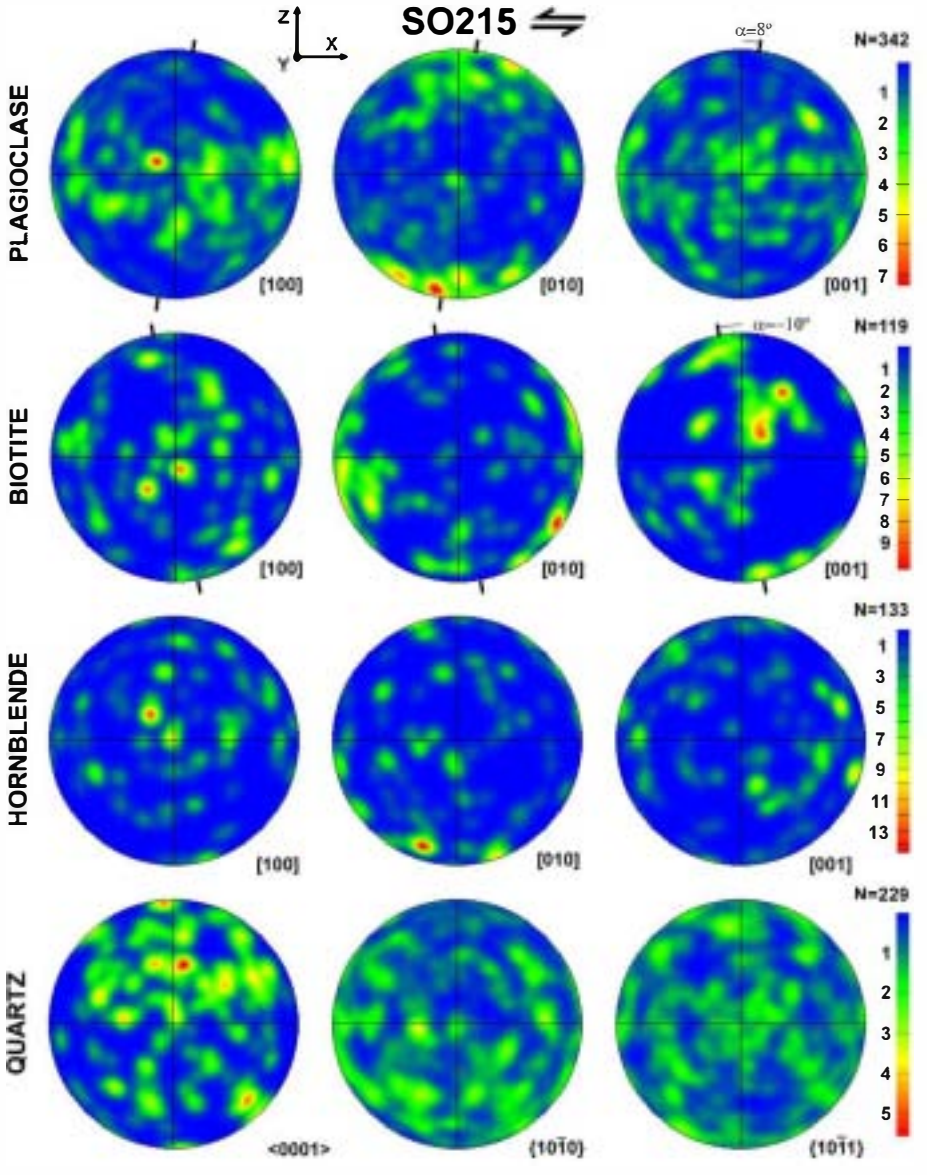

Fig. 6. Lower hemisphere equal-area projections of the CPOs of plagioclase, biotite, hornblende and quartz for the samples SO215 (subvertical domain) obtained by EBSD. The plane XY corresponds to the measured mesoscopic foliation and X to the horizontal line inside the foliation. The α angle of plagioclase and biotite are indicated. *N* is the number of EBSD measurements. The units of the scale bars are multiples of random distribution.

the foliation plane presents $R = 1.086$ (R is the eccentricity of the shape fabric ellipse), which indicates that the lineation is weak. The fabric is mainly planar as indicates the SPO results for the plane normal to foliation ($R = 1.267$), but the orientation of the foliation obtained by the Intercept method (shape foliation) is oblique (8.34°) in respect to the measured mesoscopic foliation. The obtained elements of the fabric L (lineation), F (pole to mesoscopic foliation), SF (pole to the shape foliation) are also represented in geographic coordinates in Fig. 3.

The results of the SPO study performed for sample SO215 are quite different (Fig. 3). The fabric in this case is planar and there is no evidence of lineation in the shape orientation of plagioclase ($R \approx 1$ in the study within the mesoscopic foliation). The study of the plane normal to foliation indicates a planar fabric less intense ($R = 1.159$) than the previous sample (SO226). Again the foliation observed by the Intercept Method (shape foliation, SF) is not exactly parallel to the mesoscopic foliation observed in the sample (F), forming both planes 14.38°.

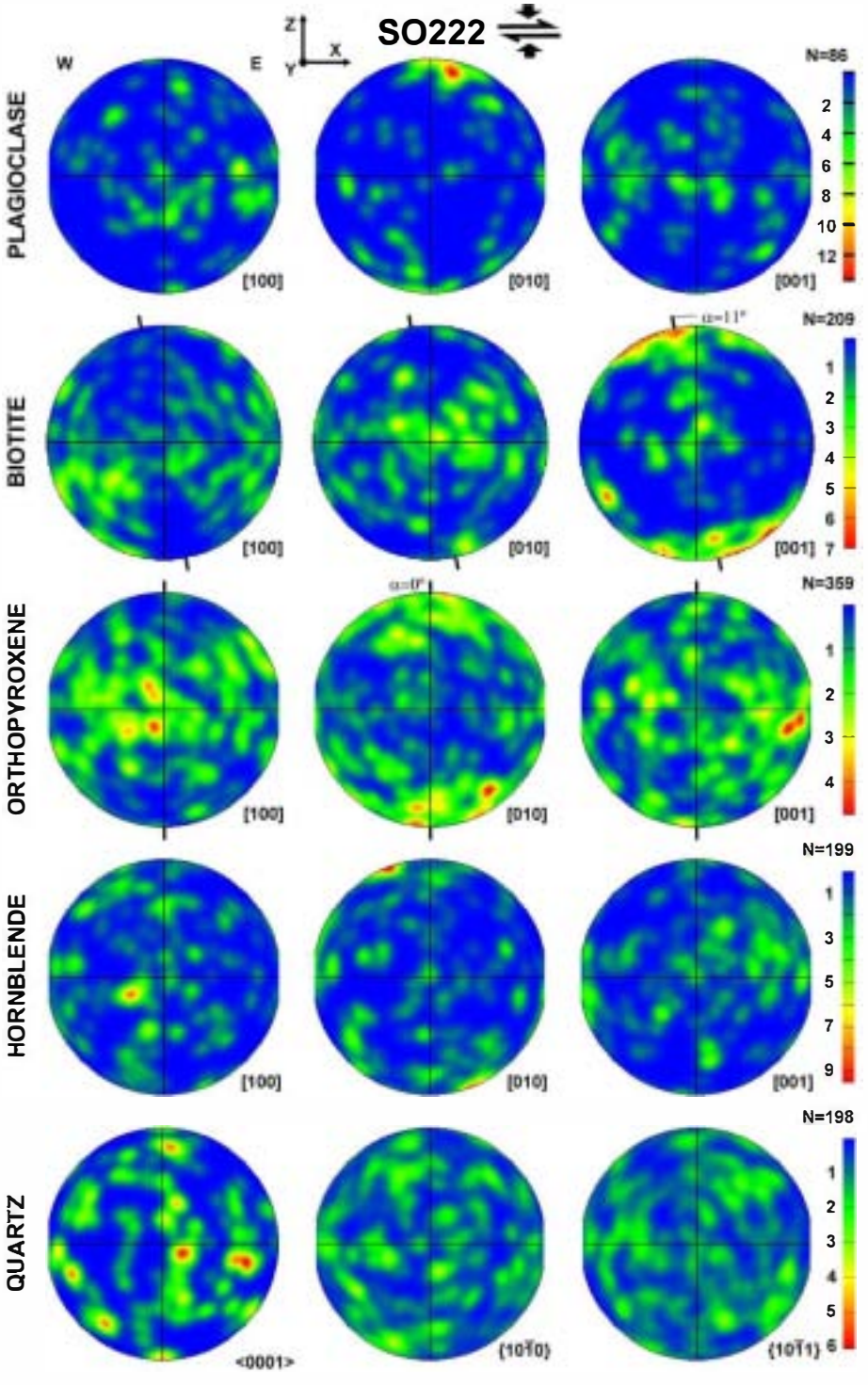

Fig. 7. Lower hemisphere equal-area projections of the CPOs of plagioclase, biotite, orthopyroxene, hornblende and quartz for the samples SO222 (subhorizontal domain) obtained by EBSD. The plane XY corresponds to the measured mesoscopic foliation and X to the lineation obtained in the SPO study of plagioclase. The α angle of biotite is indicated. *N* is the number of EBSD measurements. Note that the number of measurements on plagioclase is small compared with the other samples, due to the more mafic composition of SO222. The units of the scale bars are multiples of random distribution.

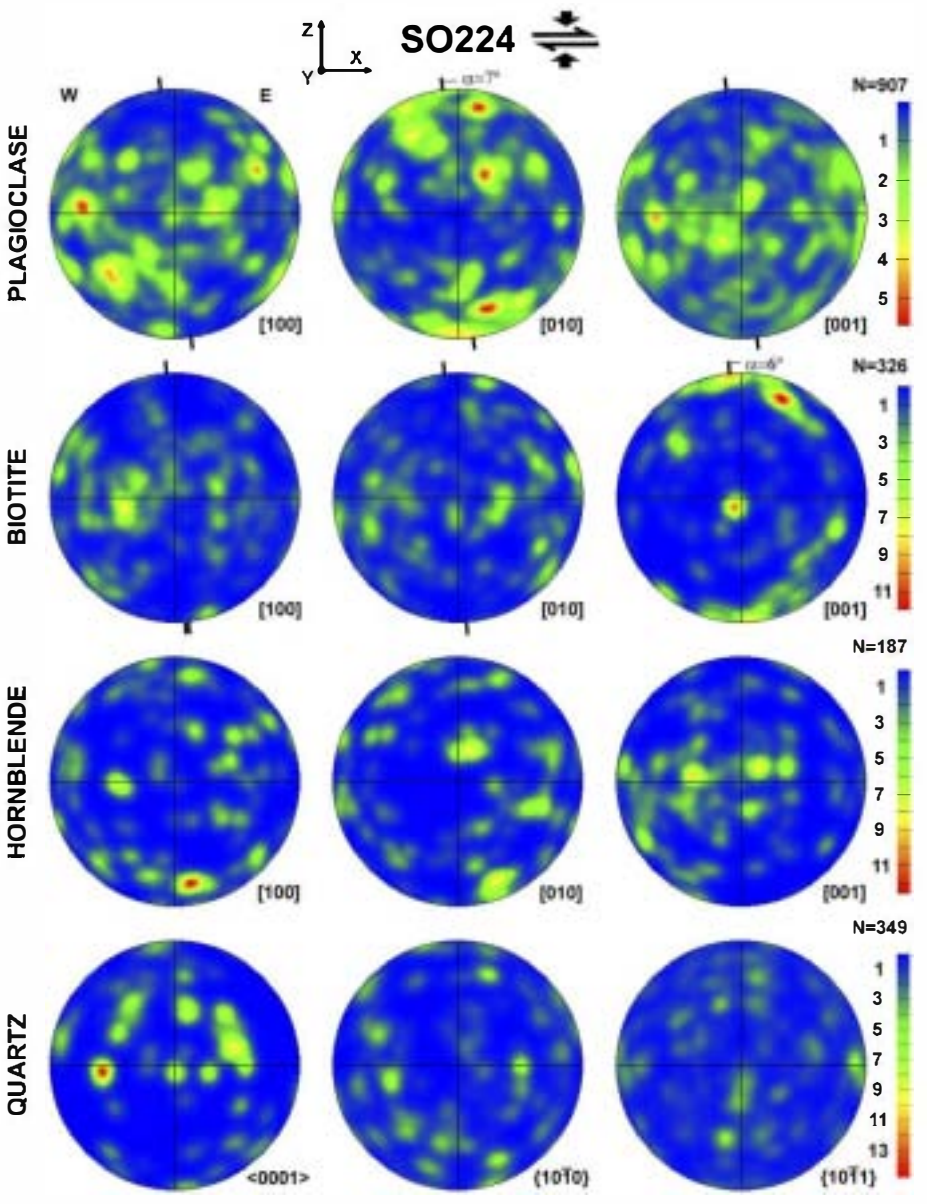

Fig. 8. Lower hemisphere equal-area projections of the CPOs of plagioclase, biotite, hornblende and quartz for the samples SO224 (subhorizontal domain) obtained by EBSD. The plane XY corresponds to the measured mesoscopic foliation and X to the lineation obtained in the SPO study of plagioclase. The α angle of plagioclase and biotite are indicated. *N* is the number of EBSD measurements. The units of the scale bars are multiples of random distribution.

4.1.2. Subhorizontal domain (SO222, SO224)

The SPO study of the samples from the subhorizontal domain has revealed, in both cases, magmatic lineations trending to the W (SO222, Fig. 4) and WSW (SO224, Fig. 4). The shape foliations evidenced by the Intercept Method in these samples are, as those samples from the subvertical domain, oblique in respect to the mesoscopic foliations, but forming smaller angles in this case (2.93° in SO222 and 0.52° in SO224). The intensity of lineations is very weak (R=1.101 for SO222 and R=1.096 for SO224) while the intensity of foliations is higher (R=1.167 for SO222 and R=1.113 for SO224). The orientation in geographic coordinates for all the fabric elements can be seen in Fig. 4.

4.2. Magmatic CPOs

The SPO analysis has identified that weak magmatic lineations were present in three of our samples. The orientation of the framework is well established for

these samples (X is parallel to the shape lineation, Z is assumed to be located in the pole of the observed mesoscopic foliation and Y is perpendicularly oriented).

The CPOs of the main mineral phases (labradorite, biotite, orthopyroxene if present, hornblende and quartz) were analyzed for each sample.

The crystallization sequence in the Santa Olalla tonalite indicated by igneous textures is: firstly plagioclase with the most euhedral morphologies, secondly orthopyroxene also with euhedral shapes (only present in sample SO222), thirdly biotite also with euhedral shapes, fourthly hornblende with anhedral shapes sometimes showing poikilitic textures and finally quartz which always shows anhedral morphologies filling porosity with poikilitic textures.

The results of the CPO study are presented in Figs. 5–8, corresponding to SO226, SO215, SO222 and SO224, respectively. The results are presented on stereo plots, with the pole to the measured mesoscopic foliation (Z) oriented N–S in the diagram, and the shape lineation (X) in the E–W direction of the diagram. The results for SO215, the sample of the subvertical structural domain that does not show shape lineation has been represented with the horizontal line within the foliation located in the E–W direction of the diagram.

4.2.1. Subvertical domain (SO226, SO215)

Plagioclase fabrics in the samples belonging to the subvertical domain are characterized a vertical magmatic foliation defined by the 010 poles (the more developed face of plagioclase growing into a liquid) which is coherent with the field observations. In detail, the 010 plagioclase poles show an asymmetric orientation with respect to Z (Figs. 5 and 6) implying a degree of crystal imbrication or tiling (Blumenfeld, 1983; Blumenfeld and Bouchez, 1988; Ildefonse et al., 1992; Arbaret et al., 1996). This imbrication can be interpreted as a sinistral simple shear strain with a horizontal direction during the generation of the vertical magmatic foliation. The 001 and 100 poles of plagioclase define a diffuse girdle perpendicular to the 010 maximum featuring no clear crystallographic lineation in the plagioclase fabric, from which it can be deduced that the shape lineation detected in sample SO226 is formed by axes 001 and 100. The biotite subfabric is more random than that of the plagioclase. While the plagioclase shows coarse euhedral grains and a clearly planar igneous fabric, the biotite with a smaller size and more isometric shapes show an intriguing and complex CPO. The 001 poles of biotite that define its planar habit are distributed with a girdle within XZ in SO226 (Fig. 5) completed with a concentration around Y. The biotite subfabric of SO215 is less clearly defined, although it is similar to SO226. The complex pattern of 001 poles together with the similar crystallographic development of 010 and 100 planes in biotites yield a near random orientation of the 010 and 100 poles. The CPOs of hornblende differs between the two samples SO215 and SO226. SO215 is a tonalite with a minor amount of hornblende and yields a random orientation for this mineral, indicating a late crystallization with a poikilitic texture. In contrast the hornblende in SO226 (a hornblende rich quartzdiorite) has been weakly oriented during the magmatic state, giving a soft girdle in the XY foliation plane for the long axis of hornblende prisms (001), like in the case of the plagioclase the girdle of the 001 axes of hornblende is slightly oblique to the foliation plane giving the same sinistral shear sense. The last mineral to crystallize was quartz, filling the gaps between other phases with poikilitic textures. Thus, both samples show a random CPO of the *c*-axes of quartz.

4.2.2. Subhorizontal domain (SO222, SO224)

These samples feature similar plagioclase CPOs to the samples from the subvertical domain. The 010 plagioclase poles clearly define the igneous foliation measured in the field. In this case, while SO222 presents an almost orthorhombic symmetry for the CPO of plagioclase (Fig. 7), SO224 shows a degree of tiling (Fig. 8) indicating a non-coaxial component of deformation giving a top to the E shear sense. In both samples the 001 and 100 plagioclase poles, are distributed with random orientations in girdles perpendicular to the 010 maximum. Consequently the contribution of 001 and 100 axes to the magmatic lineation is similar.

In contrast to the results obtained for the subvertical domain, the biotite CPOs of the samples from the subhorizontal domain are more concordant with the fabrics of plagioclase. The 001 biotite poles show the same orientation as the 010 plagioclase poles in sample SO224 (Fig. 8), and a subparallel orientation in SO222 (Fig. 7). This indicates that the preferred orientation of biotite plates also contributes to the magmatic foliation observed in the field.

The 001 biotite poles also show tiling in the same sense that was observed for the 010 plagioclase poles, in SO224 (Fig. 8); and a similar tiling in SO222, contrasting with the orthorhombic fabric of plagioclase in this sample. The tiling of biotite in both samples gives a top to the E shear sense. The 010 and 100 biotite poles define girdles perpendicular to the 001 maximum. Sample SO222 (Fig. 7) indicates that there is a difference in the orientation of 010 and 100 axes within the girdle, with the 100 axes being better oriented to the shape lineation.

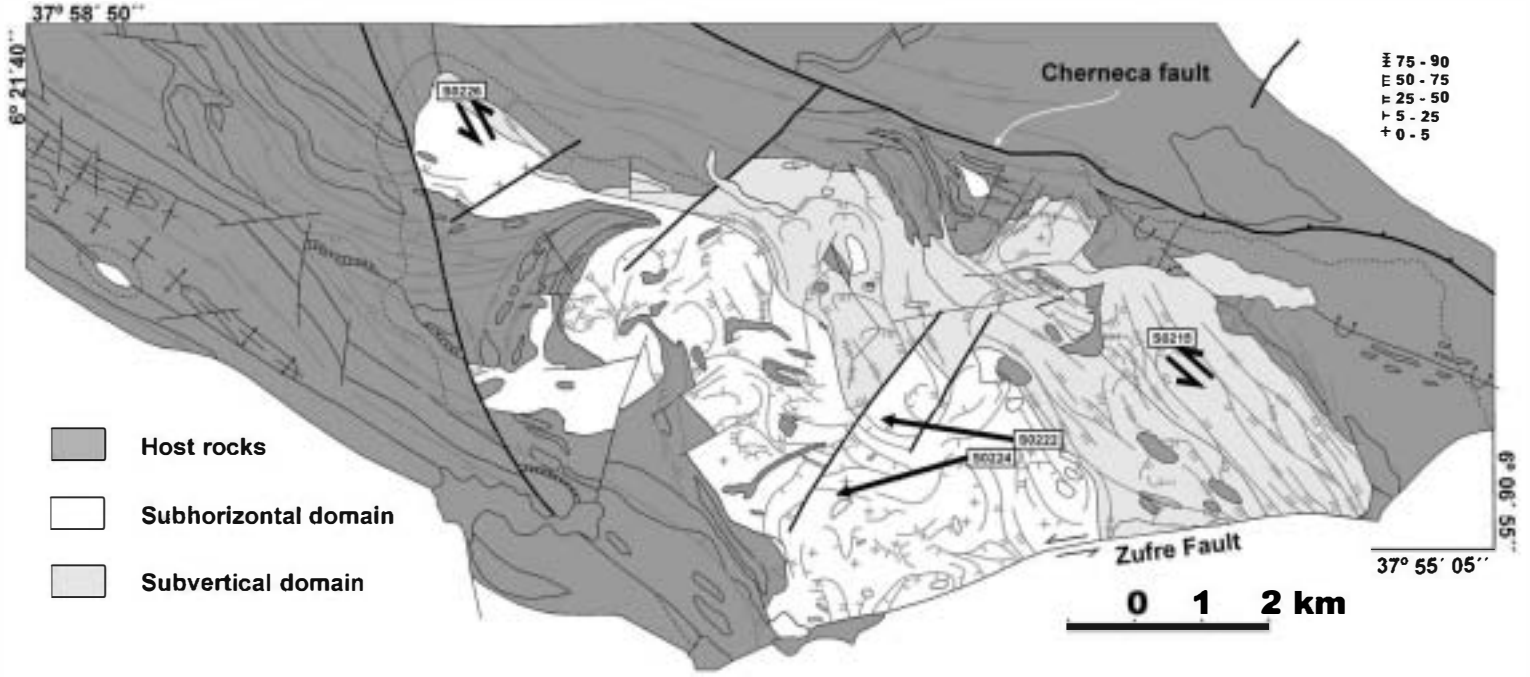

Fig. 9. Shear sense (subvertical domain) and the directions of magma flow (subhorizontal domain) obtained by the SPO and CPO study, represented on the foliation trajectory map.

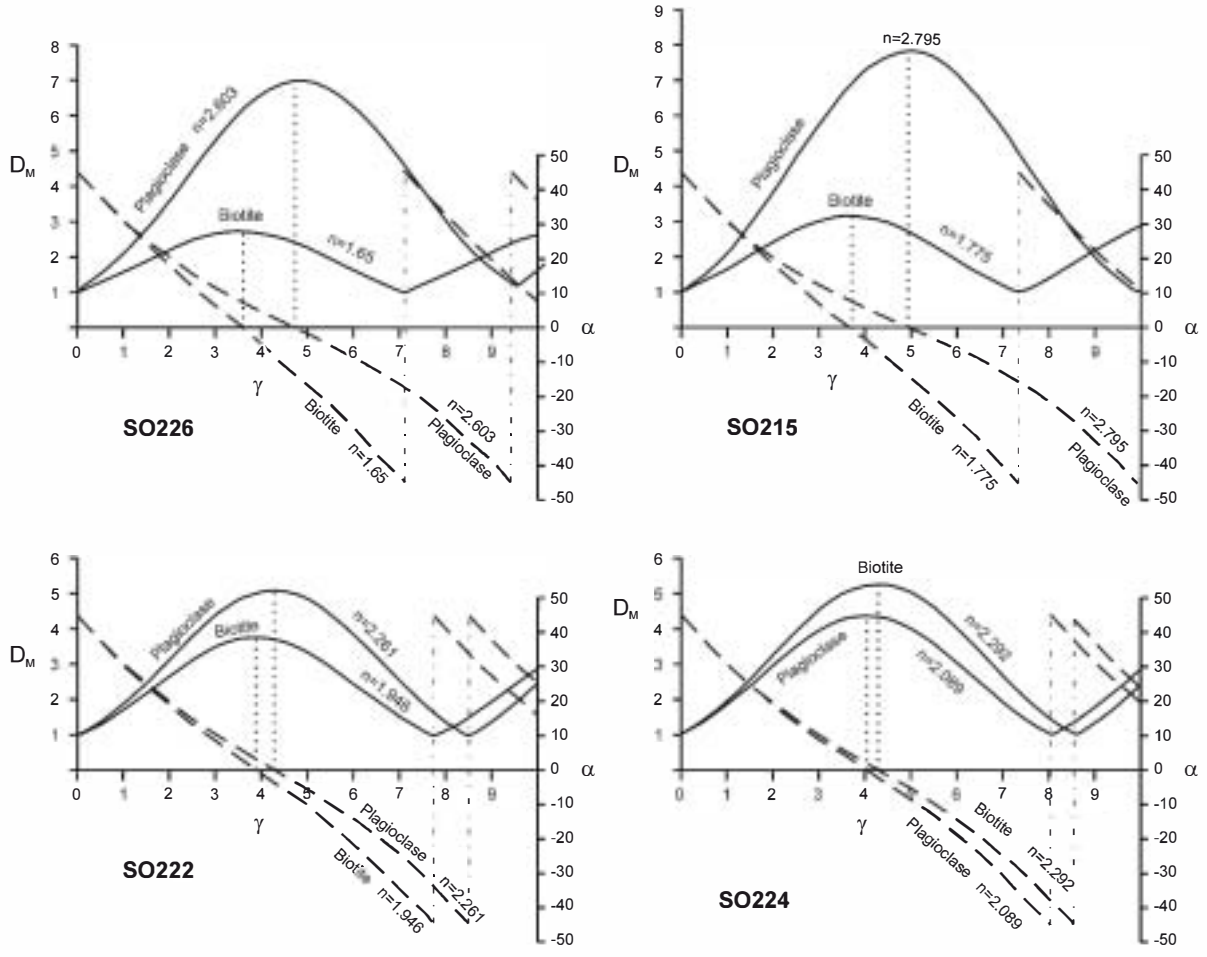

Fig. 10. Numerical modelling of the fabric evolution of plagioclase and biotite for all the samples.

SO222 is the only sample that presents a significant amount of orthopyroxene. This phase starts to crystallize in the first places, when a large amount of liquid is still present and consequently the formation of a magmatic fabric by this mineral is possible. The CPO of orthopyroxene in SO222 is very strong. It is characterized by an orthorhombic symmetry with the 010 poles aligned on Z, defining the mesoscopic magmatic foliation. The 001 and 100 axes are distributed in a girdle within the foliation, with stronger maxima in the shape lineation (X) for the 001 axes (which correspond to the elongation of prisms) and in the Y direction for the 100 poles.

The long axes of the hornblende prisms (001) are distributed with random orientations although the highest density can be observed in a wide girdle containing the XY foliation plane (especially clear for SO222, Fig. 7). The random CPOs of quartz (Figs. 7 and 8) reflect, as in the samples from the subvertical domain, that this mineral is the last one to crystallize.

5. Discussion

The SPO study of plagioclase grains has served to reveal the presence of weak magmatic lineations, but also has served to evaluate the intensity of the planar fabric. The foliation measured at the mesoscale does not completely fit with the orientation of the foliation detected by the Intercept Method. This can be interpreted as being caused by a tiling of the plagioclase grains oriented during a non-coaxial deformation. The mesoscale foliation can be assumed as the general flow plain, but the detailed shape study reveals an oblique orientation of the shape foliation caused by a tiling of the crystals, indicative of a shear sense for each sample. The obtained shear sense for each sample is indicated in the stereo plot of the fabric

elements in geographic coordinates shown in Figs. 3–4. This interpretation of the monoclinic symmetry of the SPO is supported by the fact that the results are completely coherent with the interpretation of the emplacement mechanisms and tectonic evolution of the SOIC proposed by Romeo et al. (2006b). The samples from the subhorizontal domain show a top to the W shear sense. Taking into account that the SOIC is only incipiently eroded can be considered that the non-coaxial deformation during the generation of the subhorizontal domain was caused by a drag against the upper boundary of this tabular intrusion. This interpretation allows us to infer that the plagioclase tiling in both samples (SO222 and SO224, top to the E) indicate a westwards magma entering. These inferred flow directions (parallel to the shape lineation) are indicated in Fig. 9 and are coherent with the entrance of magma from the roots obtained by gravity modelling (Romeo et al., 2006b). The samples from the subvertical domain also show a monoclinic SPO caused by plagioclase tiling indicating a sinistral non-coaxial deformation in magmatic state (Fig. 3). These results are coherent with the proposed tectonic origin of the subvertical domain as caused by the sinistral deformation in the magmatic state. This was promoted by the Cherneca fault strain field, an interpretation initially based on the S–C structures shown in the foliation trajectory map (Fig. 2) and the presence of vertical corridors cross-cutting previous subhorizontal foliations (Romeo et al., 2006b). The shear sense obtained by the monoclinic symmetry of the subvertical domain samples (sinistral) is also shown in Fig. 9.

The relationship between the fabrics of each mineral phase obtained by EBSD is complex. Plagioclase, biotite and orthopyroxene (when present) are the main fabric-forming minerals, and hornblende plays a role during fabric generation only in the more mafic samples (quartzdiorites), while quartz is always the last main phase to crystallize and consequently shows random orientations. The subhorizontal domain displays a parallelism between the preferred orientation of plagioclase and biotite, contrasting with the subvertical domain which shows very different CPOs for these phases.

The subvertical domain features a foliation defined by 010 plagioclase poles in Figs. 5 and 6 with a degree of tiling consistent with a genesis by sinistral shearing, this is a new determination of the same tiling observed in the SPO study (Fig. 3). Plagioclase as the main flat-shaped mineral underwent rotation under a non-coaxial strain until the interactions between grains stabilized the observed imbricated fabric. Nevertheless the biotite, with its smaller size, shows a more complex CPO (Figs. 5 and 6). These biotite CPOs are characterized by a girdle of 001 poles in the XZ plane and a concentration around the Y direction. Small biotite grains can rotate under non-coaxial deformation between the main plagioclase crystals giving the observed XZ girdle of 001 poles. 2D analogue simulations of magmatic type simple shear with two sizes of grains shows that the larger phase is well oriented with a tiling consistent with the shear sense while the smaller phase is near randomly oriented in the XZ plane (See Fig. 9 of Ildefonse et al., 1992). In natural samples it has been demonstrated that size is related to the degree of fabric anisotropy of each phase, for example Arbaret et al. (2000) describe a more pronounced SPO anisotropy for K-feldspars phenocrysts than smaller biotite crystals in the same granite.

In the samples from the subvertical domain the concentration of 001 biotite poles around Y can be interpreted as a relict fabric. These biotites are horizontally disposed and are subparallel to the plagioclase and biotite fabrics of the adjacent subhorizontal domain. A partial reorientation of this horizontal fabric under simple shear conditions during the magmatic stage could explain the complex biotite CPO patterns observed. During sinistral shearing, the initially horizontal biotite plates with 001 poles around Y, start to rotate following a spiral path until reaching the XZ plane. Similar spiral paths were obtained by Launeau (2004) by modelling the evolution of previous fabrics reworked under simple shear. This sinistral shearing could completely rework the plagioclase fabric due to its bigger size, which implies more interactions allowing the stabilization of an imbricated fabric, whereas the reorientation of a smaller phase as biotite was only partial before final crystallization.

The foliations of the subhorizontal domain are also defined by the 010 plagioclase poles. In SO224 the plagioclase displays a degree of tiling indicating a simple shear component of strain (Fig. 8). The small amount of plagioclase in SO222, caused by the presence of orthopyroxene, gives a less defined CPO for plagioclase (N=86) (Fig. 7) and consequently we are not convinced if there is a degree of tiling in this CPO. However, the small tiling described by the SPO study is coherent with the tiling observed in the CPO of SO224, all indicating a down to the W shear sense. Considering this, the most probable origin of the igneous foliation during the entrance of magma into the tabular intrusion creating the subhorizontal domain was magmatic flow, which is consistent with a non-coaxial flow caused by drag towards the upper contact with the host rocks. In contrast to the biotite CPOs of the subvertical domain, the biotites in the subhorizontal domain display similar CPOs to plagioclase, indicating that free rotation of smaller phases was not allowed during shearing in this

domain, which could indicate a significant flattening towards the upper horizontal boundary during emplacement. Hence, the most likely interpretation for the origin of the subhorizontal fabrics is a combination of simple shear with pure shear. This is not unlikely if we consider that during the swelling of any pluton (whether this occurs passively or not) magma has to enter at the same time that the cavity is generated, which necessarily causes a dragging of magma towards the boundaries accompanied by flattening parallel to the boundaries caused by the confining pressure.

6. Numerical modelling

A 2D numerical modelling based on the formulation of Jeffery (1922) for rotation of rigid ellipsoids floating into a melt under simple shear conditions has been applied to the particular cases of our samples. The theory was generalized by Willis (1977) for arbitrary shaped particles. The solution for 2D simple shear was analyzed by Fernandez et al. (1983) and supported with analogue experiments.

The curves describing the evolution of the fabric in terms of D_M (intensity of the strain ellipse) and α (angle of the X axis of the strain ellipse and the shear plane) with respect to γ (shear strain) for each particular sample have been obtained by measuring the value of n (aspect ratio) for plagioclase and biotite on the XZ plane. The parameter n has been obtained from the average aspect ratio of all the grains present in each sample. For details of how to generate the curves see Fernandez et al. (1983). We have applied this model to our samples, and this has yielded a very useful technique for evaluating how some complex textures can be formed (for instance it can explain the opposite sense of tiling of different phases in the same sample).

The models describe the periodical evolution of the fabric suffering a simple shear flow. It starts with a random initial orientation of the grains ($D_M=1$), the intensity of the fabric increases with a progressive reduction of the positive values of α until the fabric gets parallel to the flow plane ($\alpha=0$) and the intensity is maximum ($D_M=\max$). Later, α reaches negative values indicating a monoclinic symmetry opposite to the shear sense, the fabric intensity decreases and becomes random, starting a new cycle again. The periodicity of the fabric evolution cycle only depends on the aspect ratio (n) of the grains. As plagioclase and biotite have very different aspect ratios, there is always a lag of the fabric evolution cycle between both minerals.

The models calculated for the samples of the subvertical domain are shown in Fig. 10. The angles between the shear plane (XY) and the 010 plagioclase planes and 001 biotite planes can be obtained from the CPOs (α angles). For S0226 the α angle of plagioclase is 8° indicating a $\gamma=3.5$ (Fig. 10), while the complex biotite CPO does not show a preferred α angle. For S0215 (Fig. 6), opposite α angles for plagioclase ($\alpha=8°$) and biotite ($\alpha=-10°$) can be appreciated. This apparently complex relationship between the CPO of plagioclase and biotite becomes clarified by the numerical model (Fig. 10). The different aspect ratio of plagioclase with respect to biotite generates a faster evolution of the biotite fabric in this sample which has reached negative α values, while plagioclase α values remain positive. The measured values are coherent in the model with a $\gamma\approx4$ (Fig. 10). Arbaret et al. (1996) demonstrated using analogue modelling the validity of the theory for γ values from 0 to 5, but for greater values, the number of interacting neighbouring crystals dramatically increases yielding results far from theoretical prediction. Taking into account that the samples were selected because of their high intensity fabrics, the value of $\gamma\approx4$ determined for S0215 cannot be extrapolated to the entire subvertical domain, because strain is heterogeneous and this sample probably belongs to a highly deformed corridor where γ presents a maximum.

Sample S0222 shows a less defined CPO for plagioclase (Fig. 7) from which we cannot deduce any α angle. This was probably caused by the presence of the orthopyroxene in this sample, with an orthorhombic symmetry in respect to framework defined by the mesoscopic foliation and the SPO lineation. Nevertheless, biotite shows a very well defined tiling of plagioclase with a positive value (considered positive because the tiling of biotite is coherent with the SPO monoclinic symmetry obtained for plagioclase). The biotite α angle is 11°, which indicates a shear strain $\gamma=2.8$ (Fig. 10). Sample S0224 shows a CPO with positive α angles for both plagioclase ($\alpha=7°$) and biotite ($\alpha=6°$) (Fig. 8) that are indicative of $\gamma\approx3.5$ (Fig. 10). The obtained shear strain values of the subhorizontal domain indicate moderate shearing against the upper subhorizontal contact of the intrusion due to magmatic flow during magma entrance.

The model significantly differs from reality in a number of points: (1) it considers only one aspect ratio for all the grains of a particular phase, (we have introduced an average aspect ratio, but the reality is that different aspect ratios were found for the same phase), (2) the model begins with a initial stage characterized by a random orientation of all the grains and phases, but we know that some phases start to crystallize earlier than others and probably new grains were formed during the magmatic flow or deformation, so new random grains

appeared during the shear evolution, (3) modelling does not consider the interaction between particles which is important during crystallization, (4) the model does not consider a pure shear component that probably took place in the subhorizontal domain, and (5) the model is only a 2D approximation of a 3D problem. Consequently the results obtained from the comparisons of the textures in our samples with the numerical models have to be considered qualitative rather than quantitative. Nevertheless, we consider that this comparison is very useful taking into account that the observed complex textures can be explained by the different velocity of rotation of the fabric of plagioclase and biotite, indicated by these very idealized models.

The role of biotite as a secondary fabric forming phase in plutons with mineralogies including coarser phases such as plagioclase or K-feldspar makes its CPO complex and sometimes different to the fabrics of the phenocrysts which are more easily oriented under different stress tensors. Our results clearly show that the preferred orientation of biotite is not always parallel to the main observed fabric (Figs. 5 and 6). For this reason we argue that it is unwise to rely only on biotite CPOs measured indirectly using magnetic susceptibility anisotropy in order to characterize the fabrics of plutons without taking care to compare these results with the orientation of coarser phases such as plagioclase or K-feldspar. These differences could be explained by: rotation of fine crystals under simple shear, the facility to preserve relict fabrics or a combination of both mechanisms.

7. Conclusions

Magmatic fabrics are the result of complex processes regarding magmatic flow, external tectonic strain, fluid dynamics, and the interaction between particles of different shapes and sizes included into a melt. The application of EBSD to the understanding of magmatic fabrics has been demonstrated as a very useful technique. Using this technique for analyzing the subfabric of each mineral in plutons, can be very helpful for the interpretation of fabric origin and the emplacement mechanisms.

The natural samples analyzed here demonstrate that biotite fabrics are not always good indicators of the main fabric of the rock when coarser phases such as plagioclase are present. Special care should be taken when magnetic susceptibility, which depends on the presence of paramagnetic minerals such as biotite, is the only technique used to constrain pluton fabrics in lithologies with coarser phases such as those seen in most tonalites, quartzdiorites, gabbros, and feldspar–phyric granites. A comparison of magnetic susceptibility results with the fabrics of coarser minerals is recommended, since coarser phases are better strain indicators than finer ones.

Acknowledgements

We would like to thank Patrick Launeau and Pierre-Yves F. Robin for the creation and distribution of the freeware "Intercepts 2003", allowing us an easy application of the intercept method to our samples. The research has been financed by Spanish grant PB98-0815. We would also like to thank Mike Hall, School of GeoSciences, University of Edinburgh for his time an effort in preparing the samples prior to EBSD analysis.

References

Arbaret, L., Diot, H., Bouchez, J.L., 1996. Shape fabrics of particles in low concentration suspensions: 2D analogue experiments and application to tiling in magma. Journal of Structural Geology 18, 941–950.

Arbaret, L., Fernandez, A., Jezek, J., Ildefonse, B., Launeau, P., Diot, H., 2000. Analogue and numerical modelling of shape fabrics: application to strain and flow determination in magmas. Transactions of the Royal Society of Edinburgh. Earth Sciences 90, 97–109.

Bachiller, N., Galindo, C., Darbyshire, D.P.F., Casquet, C., 1997. Geocronología Rb–Sr de los leucogranitos del complejo plutónico de Burguillos del Cerro (Badajoz). Geogaceta 21, 29–30.

Bascou, J., Camps, P., Dautria, J.M., 2005. Magnetic versus crystallographic fabrics in a basaltic lava flow. Journal of Volcanology and Geothermal Research 145, 119–135.

Benn, K., Allard, B., 1989. Preferred mineral orientations related to magmatic flow in ophiolite layered gabbros. Journal of Petrology 30, 925–946.

Bestmann, M., Prior, D.J., Veltkamp, K.T.A., 2004. Development of single-crystal s-shaped quartz porphyroclasts by dissolution–precipitation creep in a calcite marble shear zone. Journal of Structural Geology 26, 869–883.

Blumenfeld, P., 1983. Le tuilage des mégacristaux, un critére d'écoulement rotationnel pour les fluidalités des roches magmatiques. Application au granite de Barbey-Séroux (Vosges, France). Bulletin de la Société Géologique de France 7, 309–318.

Blumenfeld, P., Bouchez, J.L., 1988. Shear criteria in grante and migmatite deformed in the magmatic and solid states. Journal of Structural Geology 10, 361–372.

Casquet, C., Galindo, C., Darbyshire, D.P.F., Noble, S.R., Tornos F., 1998. Fe–U–REE mineralization at Mina Monchi, Burguillos del Cerro, SW Spain. Age and isotope (U–Pb, Rb–Sr and Sm–Nd) constrints on the evolution of the ores. GAC–MAC–APGGQ Quebec'98 Conf. Abstract 23, A-28.

Dallmeyer, R.D., García Casquero, J.L., Quesada, C., 1995. Ar/Ar mineral age constraints on the emplacement of the Burgillos del Cerro Igneous Complex (Ossa-Morena Zone, SW Iberia). Boletín Geológico y Minero 106, 203–214.

Eguiluz, L., Carracedo, M., Apalategui, O., 1989. Stock de Santa Olalla de Cala (Zona de Ossa-Morena, España). Stvdia Geologica Salmanticensia 4, 145–157.

Fernandez, A., 1987. Preferred orientation developed by rigid markers in two-dimensional simple shear strain: a theoretical and experimental study. Tectonophysics 136, 151–158.

Fernandez, A., Feybesse, J.L., Mezure, J.F., 1983. Theoretical and experimental study of fabrics developed by different shaped marckers in two-dimensional simple shear. Bulletin de la Société Géologique de France 25, 319–326.

Fliervoet, T.F., Drury, M.R., Chopra, P.N., 1999. Crystallographic preferred orientations and misorientations in some olivine rocks deformed by diffusion or dislocation creep. Tectonophysics 303, 1–27.

Iezzi, G., Ventura, G., 2002. Crystal fabric evolution in lava flows: results from numerical simulations. Earth and Planetary Science Letters 200, 33–46.

Ildefonse, B., Launeau, P., Bouchez, J.L., Fernandez, A., 1992. Effect of mechanical interactions on the development of shape preferred orientations: a two-dimensional experiment approach. Journal of Structural Geology 14, 73–83.

Jeffery, G.B., 1922. The motion of ellipsoidal particles immersed in a viscous fluid. Proceedings of the Royal Society of London 102, 161–179.

Jezek, J., Melka, R., Schulmann, K., Venera, Z., 1994. The behaviour of rigid triaxial ellipsoidal particles i viscous flows—modelling of fabric evolution in a multiparticle system. Tectonophysics 229, 165–180.

Ji, S., Jiang, Z., Rybacki, E.W.R., Prior, D., Xia, B., 2004. Strain softening and microstructural evolution of anorthite aggregates and quartz–anorthite layered composites deformed in torsion. Earth and Planetary Science Letters 222, 377–390.

Kameda, J., Yamagishi, A., Kogure, T., 2005. Morphological characteristics of ordered kaolinite; investigation using electron back-scattered diffraction. American Mineralogist 90, 1462–1465.

Kogure, T., Bunno, M., 2004. Investigation of polytypes in lepidolite using electron back-scattered diffraction. American Mineralogist 89, 1680–1684.

Launeau, P., 2004. Mise en évidence des écoulements magmatiques par analyse d'images 2-D des distributions 3-D d'orientations préférentielles de formes. Bulletin de la Société Géologique de France 175, 331–350.

Launeau, P., Robin, P.-Y.F., 1996. Fabric analysis using the intercept method. Tectonophysics 267, 91–119.

Llana-Fúnez, S., Rutter, E.H., 2005. Distribution of non-plane strain in experimental compression of short cylinders of Solnhofen limestone. Journal of Structural Geology 27, 1205–1216.

Lunar, R., Ortega, L., Sierra, J., García Palomero, F., Moreno, T., Prichard, H., 1997. Ni–Cu (PGM) mineralization associated with mafic and ultramafic rocks: the recently discovered Aguablanca ore deposit, SW Spain. In: Papunen, H. (Ed.), Mineral Deposits. Balkema, Rotterdam, pp. 463–466.

Montero, P., Salman, K., Bea, F., Azor, A., Exposito, I., González Lodeiro, F., Martínez Poyatos, D., Simancas, J.F., 2000. New data on the geochronology of the Ossa-Morena Zone, Iberian Massif. Variscan–Appalachian dynamics: the building of the Upper Paleozoic basement. Basement Tectonics 15, 136–138.

Ortega, L., Lunar, R., García-Palomero, F., Moreno, T., Martín Estevez, J.R., Prichard, H.M., Fisher, P.C., 2004. The Aguablanca Ni–Cu–PGE Deposit, Southwestern Iberia: magmatic ore-forming processes and retrograde evolution. Canadian Mineralogist 42, 325–335.

Park, Y., Means, W.D., 1996. Direct observation of deformation processes in crystal mushes. Journal of Structural Geology 18, 847–858.

Paterson, S.R., Vernon, R.H., Tobisch, O.T., 1989. A review of criteria for the identification of magmatic and tectonic foliations in granitoids. Journal of Structural Geology 11, 349–363.

Paterson, S.R., Fowler, T.K., Schmidt, K.L., Yoshinobu, A.S., Yuan, E.S., Miller, R.B., 1998. Interpreting magmatic fabric patterns in plutons. Lithos 44, 53–82.

Pennock, G.M., Drury, M.R., Spiers, C.J., 2005. The development of subgrain misorientations with strain in dry synthetic NaCl measured using EBSD. Journal of Structural Geology 27, 2159–2170.

Pignotta, G.S., Benn, K., 1999. Magnetic fabric of the Barrington Passage pluton, Meguma Terrane, Nova Scotia: a two-stage fabric history of syntectonic emplacement. Tectonophysics 307, 75–92.

Piña, R., Lunar, R., Ortega, L., Gervilla, F., Alapieti, T., Martínez, C., 2006. Petrology and geochemistry of mafic–ultramafic fragments from the Aguablanca Ni–Cu ore breccia, Southwest Spain. Economic Geology 101, 865–881.

Prior, D.J., Boyle, A.P., Brenker, F., Cheadle, M.C., Day, A., López, G., Peruzzo, L., Potts, G.J., Reddy, S., Spiess, R., Timms, N.E., Trimby, P., Wheeler, J., Zetterström, L., 1999. The application of electron backscatter diffraction and orientation contrast imaging in the SEM to textural problems in rocks. American Mineralogist 84, 1741–1759.

Romeo, I., Lunar, R., Capote, R., Quesada, C., Dunning, G.R., Piña, R., Ortega, L., 2006a. U/Pb age constraints on Variscan Magmatism and Ni–Cu–PGE metallogeny in the Ossa-Morena Zone (SW Iberia). Journal of the Geological Society (London) 163, 837–846.

Romeo, I., Capote, R., Tejero, R., Lunar, R., Quesada, C., 2006b. Magma emplacement in transpression: the Santa Olalla Igneous Complex (Ossa-Morena Zone, SW Iberia). Journal of Structural Geology 28, 1821–1834.

Romeo, I., Capote, R., Lunar, R., 2007a. Crystallographic preferred orientations and microstructure of a Variscan marble mylonite in the Ossa-Morena Zone (SW Iberia). Journal of Structural Geology 29, 1353–1368.

Romeo, I., Tejero, R., Capote, R., Lunar R., in press. 3D gravity modelling of the Aguablanca Stock, tectonic control and emplacement of a Variscan gabbronorite bearing a Ni–Cu–PGE ore, SW Iberia. Geological Magazine.

Tikoff, B., Teyssier, C., 1994. Strain and fabric analyses based on porphyroclast interaction. Journal of Structural Geology 16, 477–491.

Tornos, F., Casquet, C., Galindo, C., Canales, A., Velasco, F., 1999. The genesis of the variscan ultramafic-hosted magmatic Cu–Ni deposit of Aguablanca, SW Spain. In: Stanley, et al. (Ed.), Mineral Deposits: Processes to Processing. Balkema, Rotterdam, pp. 795–798.

Tornos, F., Casquet, C., Galindo, C., Velasco, F., Canales, A., 2001. A new style of Ni–Cu mineralization related to magmatic breccia pipes in a transpressional magmatic arc, Aguablanca, Spain. Mineralium Deposita 36, 700–706.

Vernon, R.H., Johnson, S.E., Melis, E.A., 2004. Emplacement-related microstructures in the margin of a deformed pluton: the San José tonalite, Baja California, México. Journal of Structural Geology 26, 1867–1884.

Willis, D.G., 1977. A kinematic model of preferred orientation. Geological Society of America Bulletin 88, 883–894.